

Disentangling the origins of branched tetraether lipids and crenarchaeol in the lower Amazon River: Implications for GDGT-based proxies

Claudia Zell,^{a,*} Jung-Hyun Kim,^a Patricia Moreira-Turcq,^b Gwenaël Abril,^c Ellen C. Hopmans,^a Marie-Paule Bonnet,^d Rodrigo Lima Sobrinho,^e and Jaap S. Sinninghe Damsté^a

^aRoyal Netherlands Institute for Sea Research (NIOZ), Department of Marine Organic Biogeochemistry, Den Burg (Texel), The Netherlands

^bInstitut de recherche pour le développement (IRD), Geosciences Environnement Toulouse (GET), Environmental Research Observatory (ORE)-HYBAM (Geodynamical, hydrological and biogeochemical control of erosion/alteration and material transport in the Amazon basin), Centre IRD d'Ile de France, Bondy, France

^cLaboratoire Environnements et Paléoenvironnements Océaniques et Continentaux (EPOC), Centre National de la Recherche Scientifique, Université de Bordeaux, Talence, France

^dUnité Mixte de Recherche 5563–Geosciences Environnement Toulouse (GET), Institut de recherche pour le développement (IRD), Université de Toulouse, Toulouse, France

^eUniversidade Federal Fluminense, Department of Geochemistry, Niteroi, Rio de Janeiro, Brazil

Abstract

To trace the origin of branched glycerol dialkyl glycerol tetraethers (brGDGTs), their distribution in soils and suspended particulate matter (SPM) of Amazonian rivers and floodplain lakes (*várzeas*) was studied. Differences in distribution between river SPM and surrounding (lowland) soils suggests an additional brGDGT source to eroded soils in the lowland drainage basin. Erosion of high Andean soils (above 2500 m in altitude) has no major influence because its brGDGT distribution differs substantially from that in river SPM. Furthermore, SPM in the Tapajós River, a tributary that does not derive from the Andes, has a virtually identical brGDGT distribution to that of the Amazon main stem. The higher proportion of phospholipid-derived brGDGTs in river SPM compared to soils indicates that in situ production in the Amazon is an additional source for riverine brGDGTs. This affects the methylation and cyclization index of brGDGTs (MBT-CBT), resulting in slightly lower MBT-CBT-derived temperatures and slightly higher CBT-derived pH values, i.e., between the pH of the basin soil and that of the river. Since the difference between MBT-CBT-derived temperatures of Amazon River SPM and the surrounding soils is relatively small (2°C) compared to other aquatic systems (for lakes a difference of ~ 10°C has been observed), it might still be possible to trace large climate changes in the Amazon basin with the MBT-CBT using river fan cores. However, variations in in situ production of brGDGTs in the Amazon River over time and space have to be evaluated in the future. Likewise, in situ production may affect the application of the MBT-CBT paleothermometer in other river systems. Our results also show that crenarchaeol is primarily produced in the Amazon River and that its varying production influences the branched vs. isoprenoid tetraether (BIT) index. This indicates that the BIT index not only represents the input of soil organic carbon to the river but is also affected by in situ production of brGDGTs and crenarchaeol.

Branched glycerol dialkyl glycerol tetraethers (brGDGTs; Fig. 1) are bacterial membrane lipids that occur in soil worldwide (Weijers et al. 2006, 2007b). Nine different brGDGTs, with and without rings, have been identified (Structures I–IIIc; Fig. 1). Some acidobacterial species produce specific brGDGTs but probably do not represent the only biological source (Weijers et al. 2009; Sinninghe Damsté et al. 2011). The distribution of brGDGTs, expressed by their degree of methylation (methylation index of branched tetraether; MBT) and cyclization (cyclization index of branched tetraethers; CBT), in soil correlates with mean annual air temperature (MAAT) and soil pH (Weijers et al. 2007b). It was assumed that brGDGTs are mainly produced on land and are washed into small streams and rivers by erosion and further transported to the ocean (Hopmans et al. 2004). Subsequent research has indicated that they can be used to trace soil organic carbon (OC) from

land to the ocean (Weijers et al. 2006; Huguet et al. 2007; Walsh et al. 2008), with the help of the branched vs. isoprenoid tetraethers (BIT) index. The isoprenoid glycerol dialkyl glycerol tetraether (GDGT) used in this index is crenarchaeol, which is the characteristic membrane lipid of Thaumarchaeota (Sinninghe Damsté et al. 2002), formerly known as Crenarchaeota. Crenarchaeol is found in various terrestrial and aquatic systems (Hopmans et al. 2004; Herfort et al. 2006; Weijers et al. 2006) but typically dominates over brGDGTs in marine systems.

An initial study of Congo Fan deep-sea sediments (Weijers et al. 2007a) revealed that the MBT-CBT paleothermometer showed an integrated temperature signal of the whole drainage basin of the river system. However, various factors could potentially bias the MBT-CBT palaeothermometry. For example, when applying the MBT-CBT paleothermometer to a sedimentary record from the Amazon Fan, Bendle et al. (2010) postulated that an increased brGDGT contribution from the cold Andes region was responsible for the decrease in Holocene

* Corresponding author: claudia.zell@nioz.nl

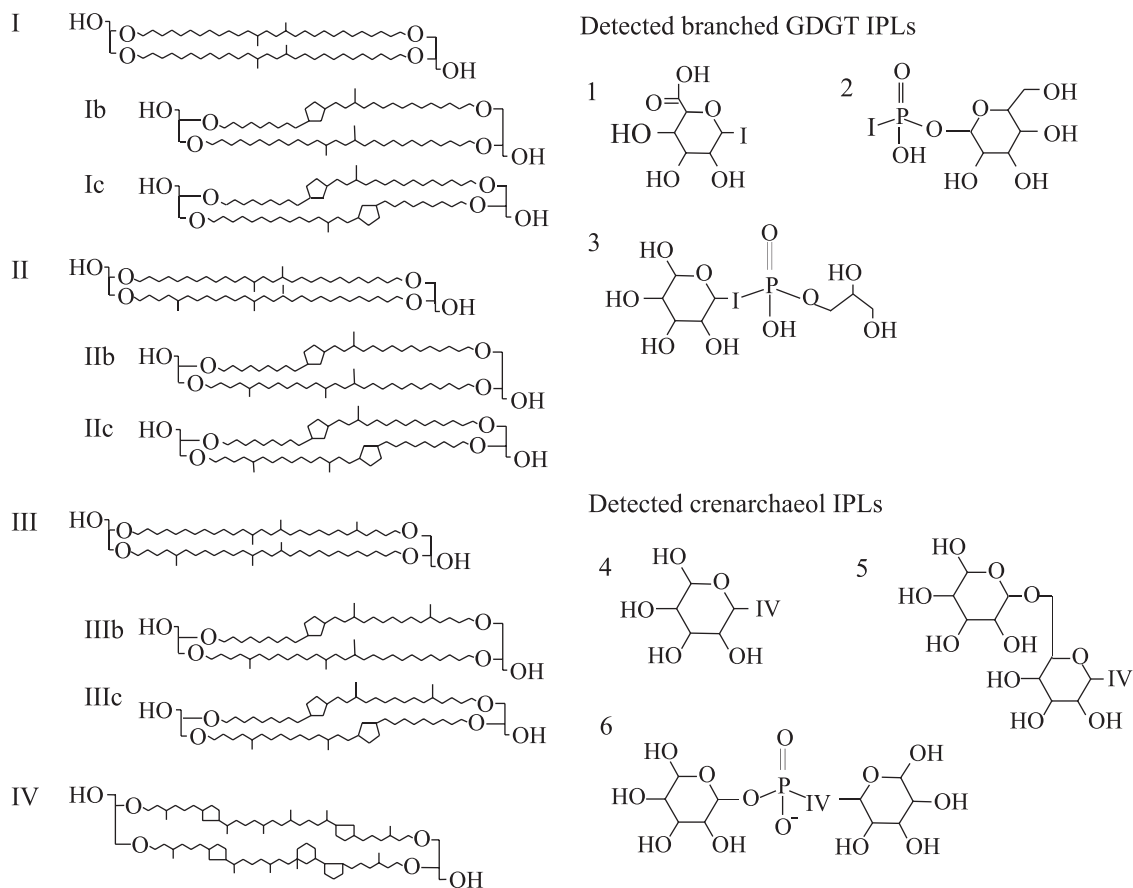


Fig. 1. Chemical structures of the brGDGT (I–IIIc) CLs, crenarchaeol CL (IV), and IPLs (1–7). The brGDGT IPLs (with brGDGT I as CL) are glyconyl-brGDGT I (1), phosphohexose-brGDGT I (2), and hexose-phosphoglycerol-brGDGT I (3). The crenarchaeol IPLs are crenarchaeol-monohexose (4), crenarchaeol-dihexose (5), and crenarchaeol-hexose-phosphohexose (6).

reconstructed temperatures. Therefore, it is essential to fully understand the provenance of brGDGTs brought by the river to the sea. In addition, it has recently been suggested that in situ production of brGDGTs in lakes or river channels may influence their distribution (Tierney et al. 2010, 2012; Zhu et al. 2011). This is thought to explain the substantially lower MBT-CBT reconstructed temperatures in lake surface sediments in comparison with the actual temperatures (Tierney et al. 2010). If brGDGTs are produced in situ in freshwater (including river) systems, it may also affect the application of the MBT-CBT palaeothermometer using deep-sea fan sediments and the application of the BIT index as an indicator of riverine-transported soil OC. In order to detect in situ production of brGDGTs the analysis of intact polar lipids (IPLs; Sturt et al. 2004) is deemed to be a useful tool. In living cells brGDGTs are present as IPLs, which are relatively quickly transformed after cell death into “fossil” core lipids (CLs) (White et al. 1979; Harvey et al. 1986), which are typically used in the MBT-CBT proxy. Branched and isoprenoid IPL GDGTs have recently been reported in biomass and the environment (Schouten et al. 2008; Liu et al. 2010; Peterse et al. 2011).

In this study, we investigated the sources of brGDGTs and crenarchaeol in the lower Amazon basin using both CL

and IPL-derived GDGTs. We compared the concentrations and distributions of brGDGTs and crenarchaeol in soils as well as in suspended particulate matter (SPM) of rivers and floodplain lakes (*várzeas*) along the lower Amazon River (Fig. 2) and used IPL-derived brGDGTs and crenarchaeol in soils as well as river and *várzeas* SPM as an indicator of in situ production. This is the first study that thoroughly tests whether the brGDGT distribution in a river system reflects an integrated signal of the average MAAT and the soil pH of its drainage basin.

Study area

The Amazon River is the largest drainage system in the world in terms of discharge and catchment area. With an area of 6,915,000 km², it covers about 40% of the South American continent (Goulding et al. 2003). Due to the equatorial position, temperature in the drainage basin is relatively constant year-round with a MAAT of ~ 26°C (Fig. 2B; New et al. 2002). Only in the Andes colder temperatures are found, due to their high elevation (Fig. 2A). The majority of soils in the lower Amazon basin are Ferralsol and Acrisol, which are both iron-rich, nutrient-poor, and acidic soil types (Quesada et al. 2009). In the Andes, patches of alkaline soils can be found (Fig. 2C).

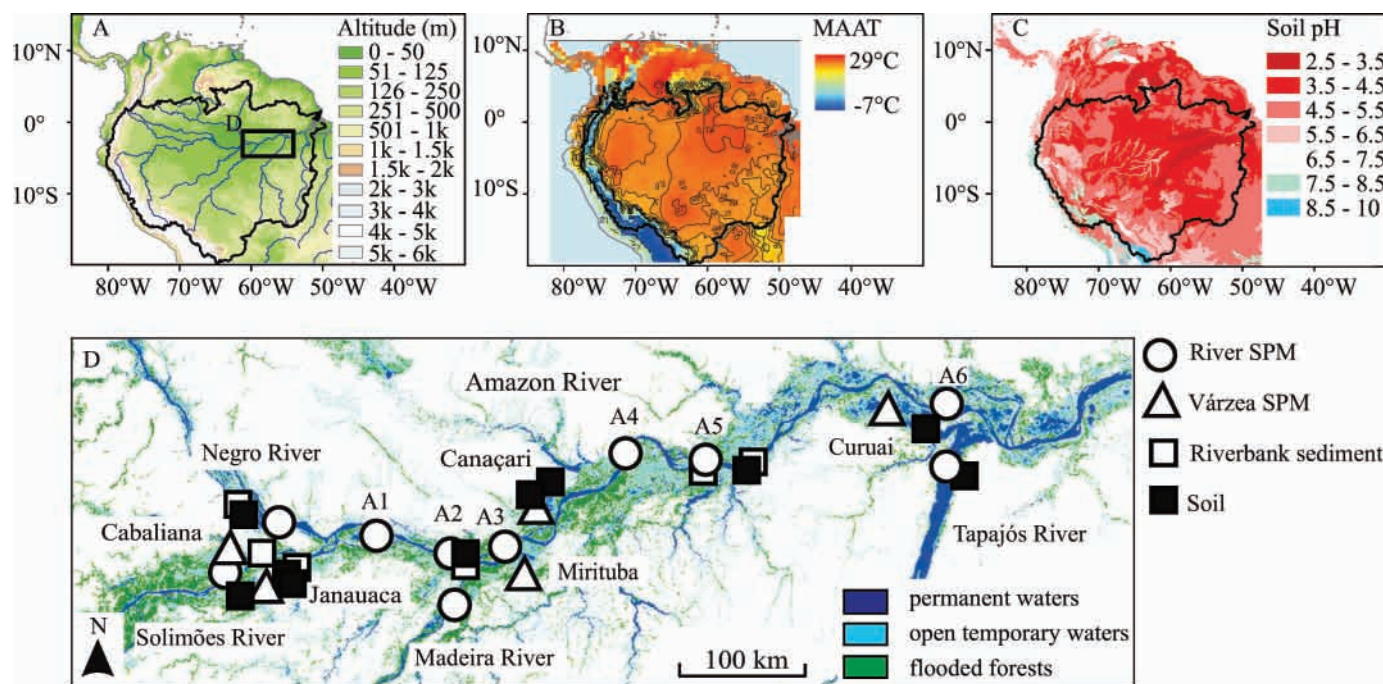


Fig. 2. (A) Map of the Amazon basin showing the Amazon watershed (black line) and the sampling area (black square). (B) MAAT in the Amazon basin (redrawn from New et al. 2002). (C) pH of 20 cm top soil in the Amazon basin (redrawn from Batjes 2005). (D) Detailed map (adapted from Martinez and Le Toan 2007) showing sample locations for soil, riverbank sediment, and SPM from rivers and *várzeas*.

The physicochemical characteristics of the Amazonian rivers reflect the soil properties of their drainage region (Konhauser et al. 1994). The biggest tributaries of the Amazon River, i.e., Solimões and Madeira, originate in the Andes. Their headwaters drain the Andean Cordillera with complex and varied lithologies, whereas their lowland portions drain fluvio-lacustrine deposits (Gaillardet et al. 1997). Solimões and Madeira are defined as “white water” rivers (Sioli 1984). According to mineralogical and isotopic evidence, the Andes is the source of 82% of the suspended particulate load exported by the Amazon River (Gibbs 1967). Due to their rich mineral content, the Andean tributaries are important to the productivity of the downstream reaches. Tributaries originating in the lowlands are typically particle and nutrient poor. In this study two tributaries originating in the lowlands were investigated: the Negro River that drains the Guyana shield and Tapajós that drains the Brazilian shield. The Negro River is a “black water” river (Sioli 1984). Dissolved humic substances are leaching from podzol found along the Negro River and lead to the typical black color of the water. The Tapajós River is a “clear water” river and characterized by a high phytoplankton production (Junk 1997). Its drainage basin has mainly Ferrasol and Acrisol (Quesada et al. 2009).

An important part of the Amazon ecosystem are the *várzeas*, which along the Amazon–Solimões corridor cover an area of $\sim 95,000$ km² (Melack and Hess 2010). Compared to the main stem, production and decomposition of organic matter is high in *várzeas* (Junk 1997). These ecosystems are strongly influenced by river dynamics and exchange waters with the main stem almost continuously

year-round. During the rainy season (rising and high water) *várzeas* are flooded by several water types, of which the Amazon main stem has the biggest influence. During the dry season (low water and falling of water) the *várzeas* export water toward the main stem (Bonnet et al. 2008). Five *várzeas* were investigated in this study. Two of them are located upstream of Manaus (Cabaliana and Janauaca) and three downstream of Manaus (Mirituba, Canaçari, and Curuai) (the lakes are listed from west to east). These *várzeas* are predominantly influenced by white waters of the Solimões, Amazon, and Madeira Rivers. The two *várzeas* located upstream of Manaus are also influenced by their local drainage basin with water types closer to black or clear waters. Cabaliana is mainly influenced by water from the Solimões River but also by the Manacapuru River (a black water river). Janauaca is comparatively small and influenced by the Solimões River and its local drainage basin. Canaçari is an intermediate as it is also strongly influenced by the Urubu River (a black water river). Mirituba is flooded by a mixture of the Amazon River and the Madeira River. Curuai is the biggest *várzea* explored within this study and is influenced by the Amazon River (Bonnet et al. 2008). While the *várzeas* upstream of Manaus are surrounded by flooded forests that are relatively untouched by humans, the downstream *várzeas* are surrounded by cleared areas that are used for larger-scale farming (Fig. 2D).

Methods

Sample collection—During the CBM6 cruise in October 2009 (low-water season), soil and SPM samples were

collected along the Amazon River main stem, four tributaries (Solimões, Negro, Madeira, and Tapajós), and five *várzeas* (Cabaliana, Janauca, Mirituba, Canaçari, and Curuai) (Fig. 2D). Sampling sites are located in a gradient of decreasing flooded forest area and increasing open lake area from Cabaliana on the Solimões River to Santarem at the mouth of the Tapajós River. To determine SPM concentrations, ~ 0.5 liters of water was filtered onto ashed (450°C, overnight) and pre-weighed glass-fiber filters (Whatman GF-F, 0.7 μm, 47 mm diameter). For the GDGT analysis, about 5 liters of water were separately filtered onto ashed glass-fiber filters (Whatman GF-F, 0.7 μm, 142 mm diameter). The filters and soils were kept frozen onboard and brought to the Royal Netherlands Institute for Sea Research (NIOZ) laboratory, where they were freeze-dried.

Environmental parameters and bulk geochemical analysis—Water pH and temperature were measured in situ with a multiparameter probe (YSI® 6600V2). To determine the pH of the soil samples, a mixture of soil and distilled water 1 : 3.5 (v : v) was prepared. This mixture was left to settle for 20 min. The pH was measured with a Wissenschaftlich-Technische Werkstätten pH 315i/SET and probe pH-Electrode SenTix 41 (pH 0–14, temperature 0–80°C, stored in 3 mol L⁻¹ KCl) at NIOZ. The total organic carbon contents of the freeze-dried and decarbonated soils were analyzed in duplicate with a Thermo-Interscience Flash EA1112 Series Elemental at NIOZ with a precision of 0.2 mg C g⁻¹. Particulate organic carbon content of river and *várzea* SPM samples was analyzed using an elemental analyzer C–H–N Fisons NA-2000 at Institute for Research and Development–France with a precision of ± 0.1 mg C g⁻¹.

Lipid extraction and fractionation—The freeze-dried samples were extracted with a modified Bligh and Dyer technique (Pitcher et al. 2009). The Bligh and Dyer extracts were fractionated into CLs and IPLs. The separation was carried out on activated silica with *n*-hexane : ethyl acetate 1 : 1 (v : v) and methanol as an eluent for CLs for IPLs, respectively (Oba et al. 2006; Pitcher et al. 2009). To each fraction, 0.1 μg C₄₆ GDGT internal standard was added (Huguet et al. 2006). Two-thirds of the IPL fraction was hydrolyzed to cleave off polar head groups as described by Weijers et al. (2011). The dichloromethane (DCM) fractions were collected, reduced by rotary evaporation, and dried over a Na₂SO₄ column. CL fractions were separated into polar (DCM : methanol 1 : 1, v : v) and apolar (DCM) fractions over an activated Al₂O₃ column.

Analysis of CL and IPL-derived GDGTs—Before analysis, samples were dissolved in hexane : isopropanol 99 : 1 (v : v) and filtered using 0.45 μm polytetrafluoroethylene filters. The CL GDGTs were analyzed using high-performance liquid chromatography–atmospheric pressure positive ion chemical ionization–mass spectrometry in selected ion monitoring mode according to Schouten et al. (2007). Quantification of the GDGT compounds was achieved by comparison of peak areas with that of the C₄₆ GDGT internal standard, correcting for the different

response factors (Huguet et al. 2006). It was reported by Pitcher et al. (2009) that during the separation of CL and IPL fractions a small amount of the CL GDGTs is carried over into the IPL fraction. Therefore, it was necessary to implement a correction to calculate the amounts of CL GDGTs and IPL-derived GDGTs more accurately as described by Weijers et al. (2011).

Calculation of GDGT-based proxies—The BIT index was calculated according to Hopmans et al. (2004):

$$\text{BIT index} = \frac{[\text{I}] + [\text{II}] + [\text{III}]}{[\text{I}] + [\text{II}] + [\text{III}] + [\text{IV}]} \quad (1)$$

The roman numerals refer to the GDGTs indicated in Fig. 1. I, II, and III are brGDGTs, and IV is the isoprenoid GDGT, crenarchaeol. Additional parameters, degree of cyclization (DC; Sinninghe Damsté et al. 2009), MBT, and CBT (Weijers et al. 2007b), were calculated as follows:

$$\text{DC} = \frac{[\text{Ib}] + [\text{IIb}]}{[\text{I}] + [\text{Ib}] + [\text{II}] + [\text{IIb}]} \quad (2)$$

$$\text{CBT} = -\log\left(\frac{[\text{Ib}] + [\text{IIb}]}{[\text{I}] + [\text{II}]}\right) \quad (3)$$

$$\text{MBT} = \frac{[\text{I}] + [\text{Ib}] + [\text{Ic}]}{[\text{I}] + [\text{Ib}] + [\text{Ic}] + [\text{II}] + [\text{IIb}] + [\text{IIc}] + [\text{III}] + [\text{IIIb}] + [\text{IIIc}]} \quad (4)$$

For the calculation of pH and temperature, the regional soil calibration for the Amazon basin was used (Bendle et al. 2010):

$$\text{CBT} = 4.2313 - 0.5782 \times \text{pH} (r^2 = 0.75) \quad (5)$$

$$\text{MBT} = 0.1874 + 0.0829 \times \text{CBT} + 0.0250 \times \text{MAAT} (r^2 = 0.91) \quad (6)$$

The analytical errors were determined by duplicate measurements of 11 samples. For the concentration of the sum of brGDGTs, the analytical error was 15% for the CL GDGTs and 13% for the IPL-derived GDGTs. Crenarchaeol concentrations had a standard deviation of 13% (CL) and 16% (IPL-derived). The average standard deviations for the MBT were 0.002 (CL) and 0.019 (IPL-derived), for the DC 0.002 (CL) and 0.01 (IPL-derived), for the CBT 0.024 (CL) and 0.063 (IPL-derived), and for the BIT 0.004 (CL) and 0.022 (IPL-derived).

IPL GDGT analysis—Two soil samples (No. 1 and 8), five river SPM samples (Negro, Solimões, Tapajós, Amazon No. 4 and 6), and one *várzea* SPM sample (Curuai) were analyzed. A selective reaction monitoring (SRM) method according to Peterse et al. (2011) was used to detect brGDGT IPLs. Crenarchaeol IPLs were detected by high-performance liquid chromatography–electrospray

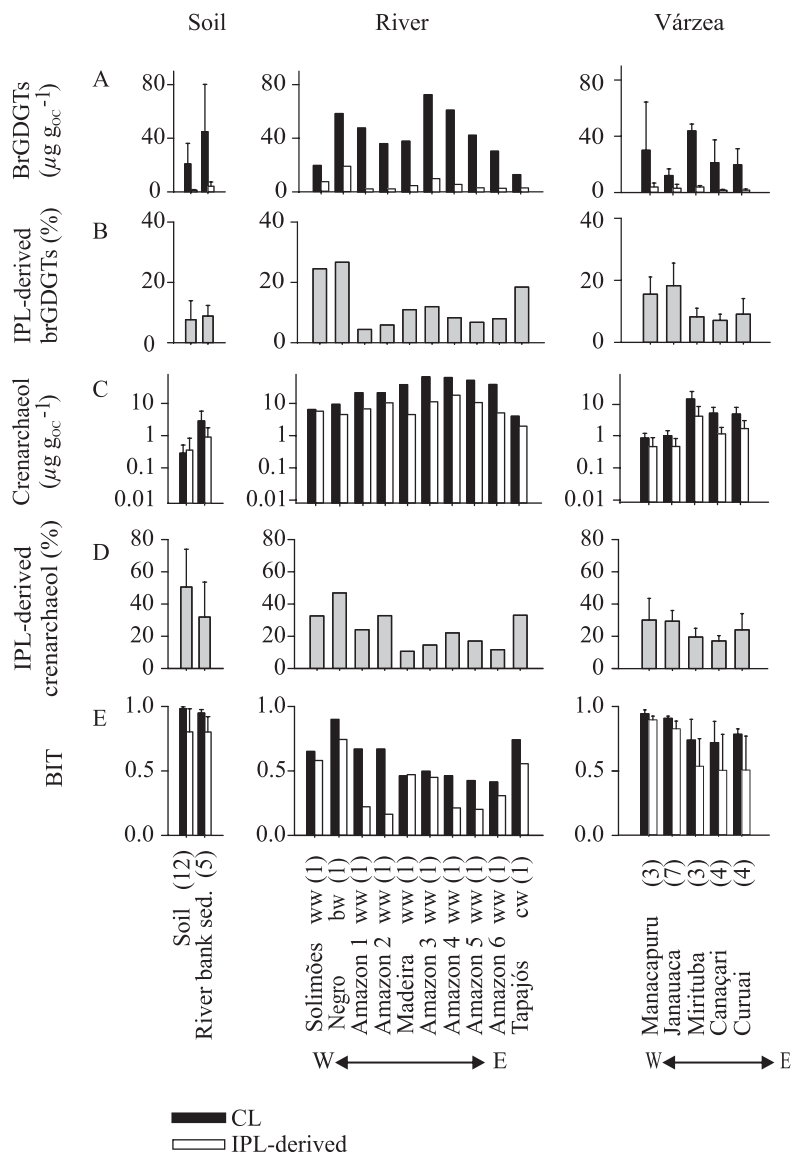


Fig. 3. (A) Concentrations of brGDGTs ($\mu\text{g g}_{\text{OC}}^{-1}$), (B) percentage of IPL-derived brGDGTs, (C) concentrations of crenarchaeol ($\mu\text{g g}_{\text{OC}}^{-1}$), (D) percentage of IPL-derived crenarchaeol, and (E) BIT index for soil and SPM from rivers and *várzeas*. The number in brackets relates to the number of samples that were analyzed. Vertical bars indicate the standard deviation (1σ). ww = white water, bw = black water, cw = clear water.

ionization–tandem mass spectrometry using an SRM method (Pitcher et al. 2011).

Results

GDGTs in soils and riverbank sediments—All soils ($n = 12$), which were never inundated by river water (i.e., collected in so-called *terra firme*), contained crenarchaeol and brGDGTs. The *terra firme* soils contained, on average, $0.3 \pm 0.2 \mu\text{g g}_{\text{OC}}^{-1}$ of CL crenarchaeol (average \pm standard deviation [1σ]). The percentage of IPL-derived crenarchaeol of the total amount of crenarchaeol was, on average, $51\% \pm 24\%$. Summed CL brGDGT concentrations were, on average, $21 \pm 15 \mu\text{g g}_{\text{OC}}^{-1}$ with $8\% \pm 6\%$

IPL-derived brGDGTs of the total amount of brGDGTs (Fig. 3). The average abundance of brGDGT I was 93% of all CL brGDGTs and 85% of all IPL-derived brGDGTs (Fig. 4A,B). The brGDGTs I, Ib, Ic, II, IIb, and III were detected in all soils, whereas brGDGT IIIb and IIIc were not detected and brGDGT IIc was found in only a few soils. The BIT index of the soils was 0.98 ± 0.01 in the CL fractions and 0.8 ± 0.2 in IPL-derived fractions (Fig. 3E). Interestingly, the soils showed a difference in CBT and MBT between the CL and IPL-derived fractions. Both CBT and MBT were slightly higher in the CL fractions (Fig. 5).

For the riverbank sediments ($n = 5$), which were underwater during the high-water seasons, the concentra-

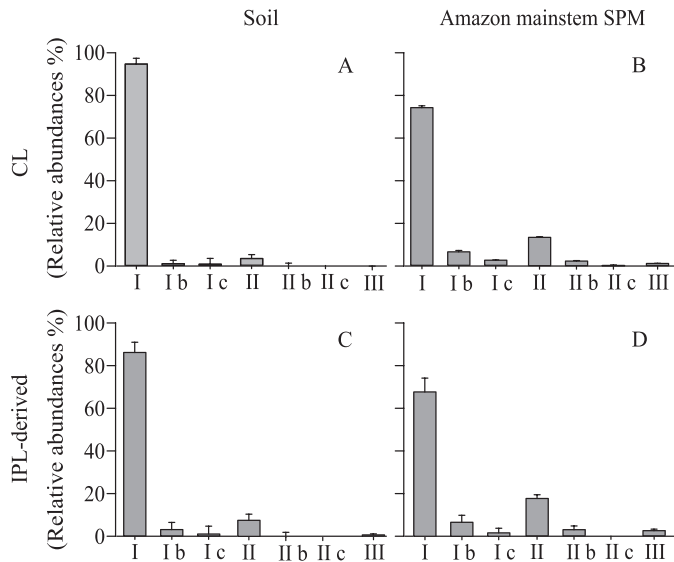


Fig. 4. Average CL and IPL-derived brGDGT distributions in 12 soil samples and in six Amazon River SPM samples. Error bars indicate the standard deviation between the measured samples.

tions of CL crenarchaeol were, on average, $2.9 \pm 2.9 \mu\text{g g}_{\text{OC}}^{-1}$, an order of magnitude higher than that of the soils. IPL-derived crenarchaeol represented $32\% \pm 22\%$ of total crenarchaeol. The concentrations of brGDGTs were similar to those of the soils with $45 \pm 35 \mu\text{g g}_{\text{OC}}^{-1}$ of which $9\% \pm 4\%$ were IPL-derived. The average abundance of brGDGT I was lower than in soil, with 77% of all CL brGDGTs and 69% of all IPL-derived brGDGTs. The riverbank sediments showed similar average BIT value as the soils: 0.95 ± 0.03 for the CL GDGTs and 0.80 ± 0.12 for the IPL-derived GDGTs (Fig. 3E).

GDGTs in river and várzea SPM—The river SPM ($n = 6$) contained the highest CL crenarchaeol concentrations with $31 \pm 23 \mu\text{g g}_{\text{OC}}^{-1}$, which is about 100 times higher than in soils (Fig. 3C; note the logarithmic scale). The concentration of CL brGDGTs was similar to that of the soils ($42 \pm 19 \mu\text{g g}_{\text{OC}}^{-1}$; Fig. 3A). The IPL percentages for crenarchaeol and brGDGTs were $23\% \pm 12\%$ and $11\% \pm 7\%$, respectively. The most abundant brGDGT was brGDGT I, but its abundance was lower than in the soils (74% and 69% of all CL and of all IPL-derived brGDGTs, respectively) (Fig. 4C,D). The average BIT was 0.60 ± 0.16 in the CL fraction and 0.4 ± 0.2 in the IPL fraction (Fig. 3E).

In SPM collected from the *várzeas* ($n = 21$), the crenarchaeol concentration was higher than that of the soils but 10 times lower compared to that of the river SPM ($5 \pm 6 \mu\text{g g}_{\text{OC}}^{-1}$; Fig. 3C). The CL brGDGT concentration was similar to that of the soils ($22 \pm 17 \mu\text{g g}_{\text{OC}}^{-1}$). The IPL percentage for crenarchaeol and brGDGTs were $25\% \pm 9\%$ and $13\% \pm 7\%$, respectively. As in the soils and river SPM, the most abundant brGDGT was brGDGT I and its average abundance was 78% and 76% of all CL and of all IPL-derived brGDGTs, respectively. Average BIT values were 0.83 ± 0.13 for the CL fractions and 0.68 ± 0.24 for the IPL-derived fractions.

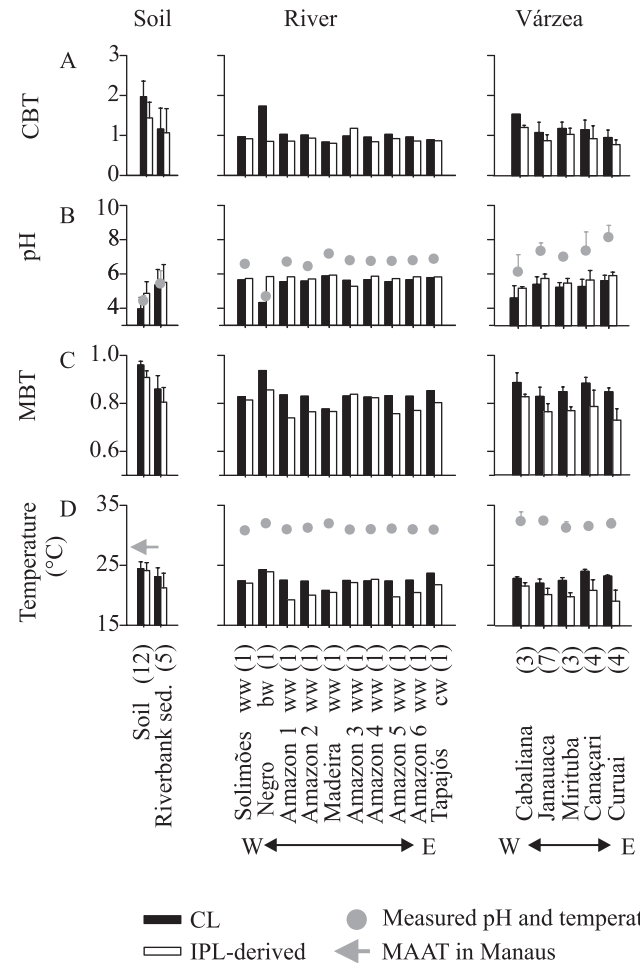


Fig. 5. (A) CBT, (B) CBT-derived pH and measured pH, (C) MBT, (D) MBT-CBT-derived MAAT, measured water temperatures, and the MAAT at Manaus. The numbers in brackets relate to the number of samples that were analyzed. Vertical bars indicate the standard deviation (1σ). sed. = sediment, ww = white water, bw = black water, cw = clear water.

IPL GDGTs—To obtain more direct evidence for the presence of IPL GDGTs, a selection of samples ($n = 8$) was analyzed for a number of known IPL GDGTs. The analyzed samples were two soil samples, five river SPM samples (Negro, Solimões, Tapajós, Amazon No. 5 and 6), and one *várzea* SPM sample (Curuai). Phosphohexose-brGDGT I (2; numerals refer to Fig. 1) and hexose-phosphoglycerol brGDGT I (3) were found in all samples. Glyconyl-brGDGT I (1) was only found in the Amazon 5 SPM sample, probably due to its low concentration. For crenarchaeol-derived IPLs the monohexose (4) and dihexose (5) were found in all samples except in the Tapajós River SPM, which lacked the dihexose. Hexose-phosphohexose (6) was detected in all samples except in the Solimões, Amazon 6, and Tapajós SPM.

Discussion

Sources of brGDGTs in river SPM—It has been assumed that the majority of brGDGTs are produced in soil and

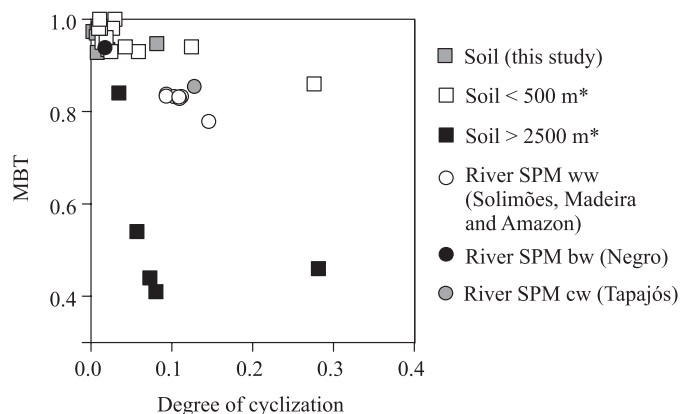


Fig. 6. Cross plot to compare the DC and MBT of CL brGDGTs from lowland and high Andean soil with those of CL brGDGTs in river SPM. The data of soil samples marked with an asterisk are from Kim et al. (2012). ww = white water; bw = black water; cw = clear water.

upon erosion of the soil are transported by rivers to the ocean (Hopmans et al. 2004; Weijers et al. 2006). Our data allow us to critically evaluate this hypothesis. Unlike crenarchaeol (*see below*), there is no significant difference in OC-normalized concentration of brGDGTs between soils and SPM in the lower Amazon basin (Fig. 3A). This could be in line with the general idea that the majority of brGDGTs in rivers are indeed derived from soil. However, our data also show that the distribution of CL brGDGTs in the lowland soils is different from that in Amazon River SPM, i.e., the abundance of brGDGT I is substantially lower (Fig. 4). In addition, the DC of brGDGTs is higher in the Amazon River SPM, whereas the MBT is lower compared to the soils (Fig. 6). The higher DC and lower MBT result in higher CBT-derived pH and lower MBT-CBT-derived MAAT values, respectively (Fig. 5B,D). Because the Andes air temperature is lower and the soil pH is higher (Fig. 2B,C), an influence of brGDGTs originating from Andes soils may explain this, as suggested previously by Bendle et al. (2010). They argued that a major part of the brGDGTs transported by the Amazon River to the Amazon deep-sea fan during the Holocene originated from Andean soils. This was based on the observation that MBT-CBT-reconstructed MAATs for the Holocene were lower than expected for the Amazon lowland.

To evaluate this possibility, a detailed comparison of the brGDGT distribution of river SPM and of soils from the lowland (< 500 m in altitude) and from the high Andes (above 2500 m in altitude) is made (Fig. 6). The additional soil data used for this comparison are from Kim et al. (2012). All soils from the lowland showed almost identical distributions even though they are from diverse areas, and they plot in the upper left corner of the diagram. Soils from the high Andes (above 2500 m in altitude) possess higher DC and lower MBT values (Fig. 6). The difference between the distributions in river SPM and the surrounding soils is larger than between river SPM and the surrounding soils (Fig. 6). This does not exclude an Andean influence on the brGDGT distribution in the lower Amazon SPM, but it reveals that the majority of brGDGTs do not originate from the high Andes.

As two of the studied tributaries (Negro and Tapajós) do not originate from the Andes, but from the lowlands, their brGDGT distributions provide interesting hints on the source of brGDGTs in the riverine SPM. The brGDGT distribution in the Negro River resembles that of lowland soils (Fig. 7), suggesting that brGDGTs in the black water river are predominantly derived from erosion of the surrounding soil. This is in line with the observation that the Negro River SPM has the highest BIT of all studied rivers, approaching that of soil (Fig. 3). The brGDGT distribution in the Tapajós River is similar to what is found in the Amazon main stem and the tributaries from the Andes (Madeira and Solimões) (Fig. 6). This indicates that the mismatch in GDGT distributions of the SPM in the white and clear water rivers and the lowland soils is unlikely to be explained by a contribution from Andes soils; there must be an additional source of brGDGTs. This suggests that brGDGTs can also be produced in situ in the river water and that this aquatic production is responsible for changing the distribution of brGDGTs derived from lowland soil.

To further investigate potential in situ production of brGDGTs in the river, IPL-derived brGDGTs were also analyzed and revealed the presence of both phospho- and glycolipids. Although the significance of IPLs as unequivocal markers for living cells is a topic of recent discussion (Lipp and Hinrichs 2009; Schouten et al. 2010; Lengger et al. 2012), it is known that glycosidic ether lipids degrade more slowly than phospholipids (Harvey et al. 1986; Lengger et al. 2012). The presence of brGDGTs containing a phospho head group thus suggests that at least part of the IPL brGDGTs in riverine SPM was freshly produced. In addition, the percentage of IPL-derived brGDGTs in soils is lower than in river SPM (Fig. 3B). Since brGDGT IPLs are produced by active microorganisms and are subsequently transformed into CLs, this seems to be in contradiction with a predominant soil origin of brGDGTs in riverine SPM. The higher percentage of brGDGT IPLs in SPM than in soil thus supports the idea of in situ production in the river water. Furthermore, IPL-derived brGDGT distributions clearly differ between soil and riverine SPM (Fig. 7B), with lower MBT and higher DC for riverine SPM, although the differences are slightly less apparent as for CLs (cf. Fig. 7A,B).

Sources of brGDGTs in várzea SPM—Both CL and IPL-derived brGDGT distributions of the *várzea* SPM samples have similar MBT and DC values compared to the river SPM samples (Fig. 7C,D). This suggests that brGDGTs in the SPM of the *várzeas* are of similar origin as those in riverine SPM (i.e., mixed origin from lowland soils and in situ production). There are some *várzea* SPM samples (i.e., from the sites Cabaliana 2, Janauaca 2, and Canaçari 1) that plot in the upper left corner of Fig. 7C close to the Negro River SPM and the lowland soils. These *várzeas* are indeed influenced by input of black water from their local watershed. The black water influence is reflected by the pH, which is lower compared to the other *várzea* sampling sites. Duncan and Fernandes (2010) defined the pH of black water as 4.5 ± 0.9 . Hence, only Cabaliana 2, which is

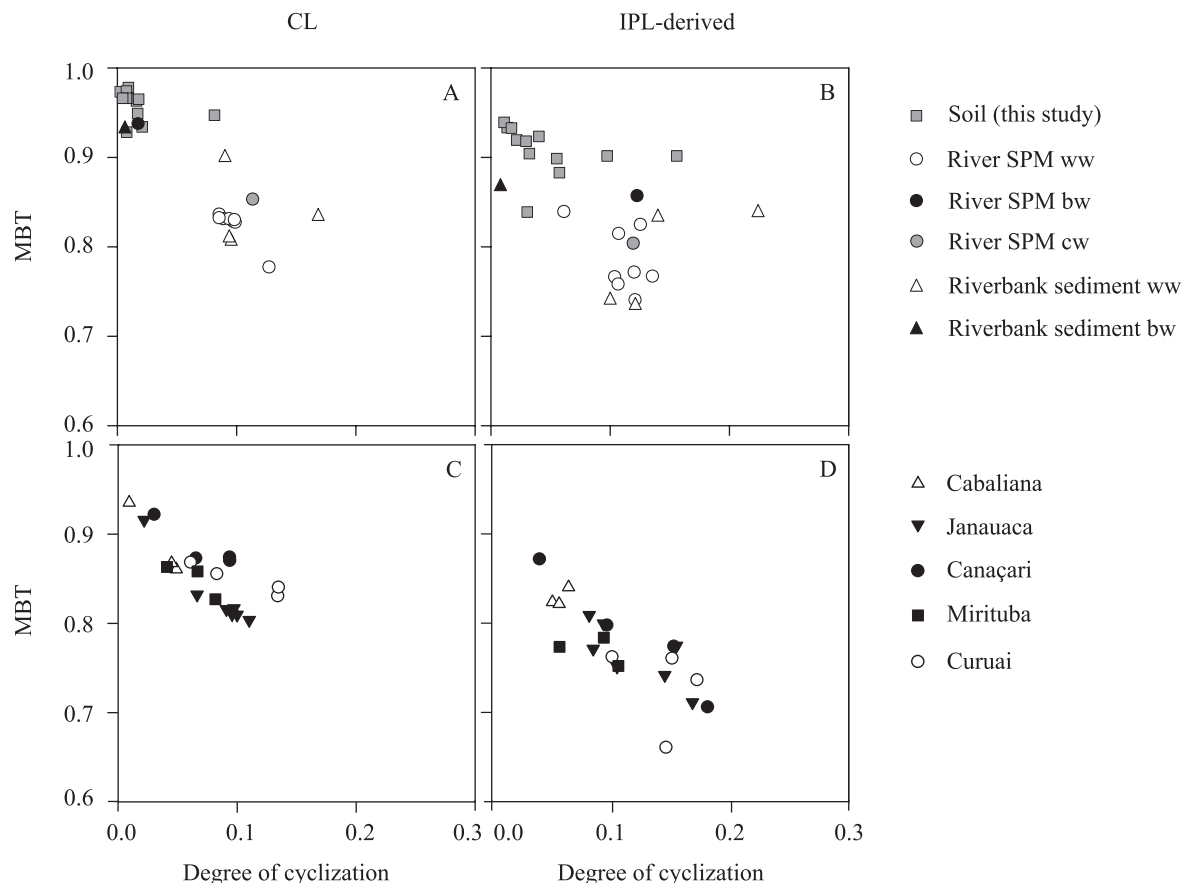


Fig. 7. Cross plot to compare the distributions of CL and IPL-derived brGDGTs in the different sample types, using the degree of cyclization (DC) and MBT. (A, B) soil, river SPM, and riverbank samples, and (C, D) *várzea* samples. ww = white water; bw = black water; cw = clear water.

substantially influenced by the Manacapuru River, falls into this range. The other two sites have slightly higher pH values but still lower than the other sites in the *várzeas*. As brGDGTs containing a phospho head group were also detected in *várzea* SPM, it seems likely that the *várzeas* are also contributing to the in situ aquatic production of brGDGTs. However, from our data it is difficult to estimate the relative importance of brGDGTs produced in the *várzeas* compared to the Amazon main stem. More data from different seasons and data from *várzea* channels connecting the rivers and the *várzeas* including flux data are required for this.

Implications for the MBT-CBT paleothermometer—The CBT-derived pH calculated for our set of lowland soils using the regional Amazon soil calibration by Bendle et al. (2010) and the measured soil pH are comparable (Fig. 5B). However, the MBT-CBT-derived temperatures (Fig. 5D) were 3°C colder than the MAAT in Manaus (MAAT measured over the last 100 yr by the World Meteorological Organization at Sta. 823310 is 26.7°C). The 3°C difference is within the 5°C calibration error range of the MBT-CBT proxy using the global soil calibration (Weijers et al. 2007b), but since a regional soil calibration was used a lower calibration error would be expected. A possible reason for this cold bias could be that the soils used to

make the regional calibration were predominantly taken in the western part of the Amazon basin (Bendle et al. 2010), which might not have been representative of the whole basin.

In the SPM of the Amazon main stem the CBT-derived pH was on average 5.6, which is between the pH of the soils (on average 4.4) and the pH of the river water (on average 6.7). This supports the idea that brGDGTs in the river are a mixture of brGDGTs produced in soil and in the river. The MBT-CBT-derived temperature using SPM was 5°C lower than the MAAT at Manaus and 2°C lower than the MBT-CBT-reconstructed temperature of the surrounding lowland soils ($24 \pm 3^\circ\text{C}$) (Fig. 5D). In comparison with several recent studies on lakes, the difference between MBT-CBT-derived temperatures of Amazon River SPM and the surrounding soils is relatively small. For example, in Sand Pond (U.S.A.), a small kettle pond, the reconstructed MAAT using CL brGDGTs in surface sediments was 12°C lower than that using soils from the watershed of the lake (Tierney et al. 2012). For Lake Towuti in Indonesia this difference was 10°C (Tierney and Russell 2009). It was suggested that this difference is due to the fact that the brGDGT-producing microbes in lakes respond differently than those in soils (Tierney et al. 2010). If we assume that brGDGT-producing microbes in the river behave similarly to those in lakes, our results suggest that in the Amazon

River the input of brGDGTs from soils is still substantially higher relative to in situ produced brGDGTs.

Our study shows that the MBT-CBT signal in the Amazon River is not substantially influenced by input of brGDGTs from the Andes, nor is it altered by the input of brGDGTs from floodplain lakes. The majority of brGDGTs in the Amazon River most likely originate from erosion of lowland soils, and to a smaller, but uncertain, extent from in situ produced brGDGTs. Application of the MBT-CBT palaeothermometer using cores from the Amazon River fan to trace long-term climatic changes of the Amazon basin may still be possible, if it is assumed that the distribution of brGDGTs produced in the river is also temperature dependent. However, we will first have to examine if in situ production of brGDGTs in the Amazon River varies over time and space. Another major question to be resolved is to what extent in situ production may influence the application of the MBT-CBT palaeothermometer in other river systems.

Crenarchaeol production in rivers and várzeas: Implications for the BIT index—Our results show that river and várzea SPM contain about 100 times higher CL and IPL-derived crenarchaeol concentrations (normalized to OC) compared to the surrounding soils (Fig. 3C). This indicates that crenarchaeol is mainly, but not exclusively produced in the aquatic system. The presence of phospho-IPLs with crenarchaeol as CLs in the SPM confirms in situ production of crenarchaeol in the aquatic system. The crenarchaeol concentration in the Amazon main stem was almost an order of magnitude higher than in the várzeas, with an average of $42 \pm 19 \mu\text{g g}_{\text{OC}}^{-1}$ in the Amazon main stem and $5 \pm 4 \mu\text{g g}_{\text{OC}}^{-1}$ in the várzeas (Fig. 3C). Therefore, it can be concluded that at the time of sampling (low-water season) a substantial amount of crenarchaeol was produced in the river itself. The percentage of IPL for crenarchaeol is higher in soils with an average of 50% compared to 20–40% in the SPM (Fig. 3B). This may reflect better preservation of the crenarchaeol IPLs in soils and possibly the difference in the suite of crenarchaeol IPLs produced in these different settings. Tierney et al. (2012) also reported a higher percentage of IPL-derived isoprenoid GDGTs in soils compared to lake sediments.

As observed for the MBT and CBT (or DC) indices, BIT values differ between the CL and IPL-derived fractions with lower values for the IPL-derived fraction (Fig. 3E). Because this difference is found in river SPM as well as in the soil samples, it might be due to a lower degradation rate in crenarchaeol IPLs compared to the brGDGTs. However, in river SPM the difference seems to be larger than in soil, which is most likely due to the relatively higher production of crenarchaeol in the Amazon River. Despite the fact that brGDGTs are also produced in the river (which would increase the BIT), the production of crenarchaeol in the river leads to substantially lower BIT values in the river (between 0.41 and 0.67) compared to the surrounding soil (average 0.98). These values represent the lowest BIT values reported for river systems (Herfort et al. 2006; Kim et al. 2007; Zhu et al. 2011). However, the rivers investigated so far are much smaller than the Amazon, and are therefore likely to be much less influenced by in situ production of

crenarchaeol. For example, SPM of the Têt River in France has an average BIT value of 0.8. However, locally it has lower BIT values (down to 0.6), which has also been explained by crenarchaeol production in the river (Kim et al. 2007). Our results indicate that within the river the BIT does not solely represent the input of soil OC, but rather reflects the production of crenarchaeol in the rivers and várzeas. The concentration of brGDGTs is likely to be a better indicator for the input of soil OC to the river; however, as shown before, brGDGTs are also partially produced in the river. Consequently, it is of utmost importance to further constrain the effect of aquatic production of GDGTs in the catchment area and its influence on the BIT index in order to use the BIT as a proxy to trace riverine or soil OC input to the ocean.

Acknowledgments

We thank three anonymous reviewers for their constructive comments. The research leading to these results has received funding from the European Research Council (ERC) under the European Union's Seventh Framework Program (FP7/2007–2013) ERC grant agreement [226600]. We thank J. Ossebaar and S. Crayford at Royal Netherlands Institute for Sea Research (NIOZ) for analytical support. This work was carried out in collaboration with the carbon cycle in the Amazon River (CARBAMA) project, funded by the French national research agency (ANR) and was conducted within an international cooperation agreement between the National Council for Scientific and Technological Development–Brazil (CNPq) and the Institute for Research and Development–France (IRD) (490755/2008-9) coordinated by G. Boaventura from the University of Brasilia (Brazil) and P. Seyler from the IRD (France).

References

- BATJES, N. H. 2005. SOTER-based soil parameter estimates for Latin America and the Caribbean (ver. 1.0). Report 2005/2. ISRIC World Soil Information.
- BENDLE, J. A., AND OTHERS. 2010. Major changes in Last Glacial and Holocene Terrestrial temperatures and sources of organic carbon recorded in the Amazon fan by the MBT/CBT continental palaeothermometer. *Geochim. Geophys. Geosyst.* **11**: Q12007, doi:10.1029/2010GC003308
- BONNET, M. P., AND OTHERS. 2008. Floodplain hydrology in an Amazon floodplain lake (Lago Grande de Curuai). *Journal of Hydrology* **349**: 18–30, doi:10.1016/j.jhydrol.2007.10.055
- DUNCAN, W. P., AND M. N. FERNANDES. 2010. Physicochemical characterization of the white, black, and clearwater rivers of the Amazon Basin and its implications on the distribution of freshwater stingrays (Chondrichthyes, Potamotrygonidae). *Pan-Am. J. Aquat. Sci.* **5**: 454–464.
- GAILLARDET, J., B. DUPRE, C. J. ALLEGRE, AND P. NÉGREL. 1997. Chemical and physical denudation in the Amazon River Basin. *Chem. Geol.* **142**: 141–173, doi:10.1016/S0009-2541(97)00074-0
- GIBBS, R. J. 1967. Geochemistry of Amazon River system: Part I. Factors that control salinity and composition and concentration of suspended solids. *Geol. Soc. Am. Bull.* **78**: 1203–1232, doi:10.1130/0016-7606(1967)78[1203:TGOTAR]2.0.CO;2
- GOULDING, M., R. BARTHEM, AND E. FERREIRA. 2003. The Smithsonian atlas of the Amazon. Smithsonian Books.
- HARVEY, H. R., R. D. FALLON, AND J. S. PATTON. 1986. The effect of organic matter and oxygen on the degradation of bacterial membrane lipids in marine sediments. *Geochim. Cosmochim. Acta* **50**: 795–804, doi:10.1016/0016-7037(86)90355-8

- HERFORD, L., S. SCHOUTEN, J. P. BOON, M. WOLTERING, M. BAAS, J. W. H. WEIERS, AND J. S. SINNINGHE DAMSTÉ. 2006. Characterization of transport and deposition of terrestrial organic matter in the southern North Sea using the BIT index. *Limnol. Oceanogr.* **51**: 2196–2205, doi:10.4319/lo.2006.51.5.2196
- HOPMANS, E. C., J. W. H. WEIERS, E. SCHEFUB, L. HERFORD, J. S. SINNINGHE DAMSTÉ, AND S. SCHOUTEN. 2004. A novel proxy for terrestrial organic matter in sediments based on branched and isoprenoidtetraether lipids. *Earth. Planet. Sci. Lett.* **224**: 107–116, doi:10.1016/j.epsl.2004.05.012
- HUGUET, C., E. C. HOPMANS, W. FEBO-AYALA, D. H. THOMPSON, J. S. SINNINGHE DAMSTÉ, AND S. SCHOUTEN. 2006. An improved method to determine the absolute abundance of glycerol dibiphytanyl glycerol tetraether lipids. *Org. Geochem.* **37**: 1036–1041, doi:10.1016/j.orggeochem.2006.05.008
- , R. H. SMITTENBERG, W. BOER, J. S. SINNINGHE DAMSTÉ, AND S. SCHOUTEN. 2007. Twentieth century proxy records of temperature and soil organic matter input in the Drammensfjord, southern Norway. *Org. Geochem.* **38**: 1838–1849, doi:10.1016/j.orggeochem.2007.06.015
- JUNK, W. J. 1997. The Central-African floodplain: Ecology of a pulsing system, ecological studies. Springer Verlag.
- KIM, J.-H., W. LUDWIG, S. SCHOUTEN, P. KERHERV, L. HERFORD, J. BONNIN, AND J. S. SINNINGHE DAMSTÉ. 2007. Impact of flood events on the transport of terrestrial organic matter to the ocean: A study of the Têt River (SW France) using the BIT index. *Org. Geochem.* **38**: 1593–1606, doi:10.1016/j.orggeochem.2007.06.010
- , AND OTHERS. 2012. Tracing soil organic carbon in the lower Amazon River and its tributaries using GDGT distributions and bulk organic matter properties. *Geochim. Cosmochim. Acta* **90**: 163–180, doi:10.1016/j.gca.2012.05.014
- KONHAUSER, K. O., W. S. FYFE, AND B. I. KRONBERG. 1994. Multielement chemistry of some Amazonian waters and soils. *Chem. Geol.* **111**: 155–175, doi:10.1016/0009-2541(94)90088-4
- LENGGER, S. K., E. C. HOPMANS, G.-J. REICHART, K. G. J. NIEROP, J. S. SINNINGHE DAMSTÉ, AND S. SCHOUTEN. 2012. Intact polar and core glycerol dibiphytanyl glycerol tetraether lipids in the Arabian Sea oxygen minimum zone: Part II. Selective preservation and degradation in sediments and consequences for the TEX86. *Geochim. Cosmochim. Acta*, **98**: 224–258, doi:10.1016/j.gca.2012.05.003
- LIPP, J. S., AND K.-U. HINRICHS. 2009. Structural diversity and fate of intact polar lipids in marine sediments. *Geochim. Cosmochim. Acta* **73**: 6816–6833, doi:10.1016/j.gca.2009.08.003
- LIU, X.-L., A. LEIDER, A. GILLESPIE, J. GRÖGER, G. J. M. VERSTEEGH, AND K.-U. HINRICHS. 2010. Identification of polar lipid precursors of the ubiquitous branched GDGT orphanlipids in a peat bog in Northern Germany. *Org. Geochem.* **41**: 653–660, doi:10.1016/j.orggeochem.2010.04.004
- MARTINEZ, J., AND T. LETOAN. 2007. Mapping of flood dynamics and spatial distribution of vegetation in the Amazon floodplain using multitemporal SAR data. *Remote Sens. Environ.* **108**: 209–223, doi:10.1016/j.rse.2006.11.012
- MELACK, J. M., AND L. L. HESS. 2010. Remote sensing of the distribution and extent of wetlands in the Amazon Basin, p. 43–59. *In* W. J. Junk, M. T. F. Piedade, F. Wittmann, J. Schöngart, and P. Parolin [eds.], *Amazonian floodplain forests: Ecophysiology, biodiversity, and sustainable management*. Springer Ecological Studies.
- NEW, M., D. LISTER, M. HULME, AND I. MAKIN. 2002. A high-resolution data set of surface climate over global land areas. *Clim. Res.* **21**: 1–25, doi:10.3354/cr021001
- OBA, M., S. SAKATA, AND U. TSUNOGAI. 2006. Polar and neutral isoprenyl glycerol ether lipids as biomarkers of archaea in near-surface sediments from the Nankai. *Org. Geochem.* **37**: 1643–1654, doi:10.1016/j.orggeochem.2006.09.002
- PETERSE, F., E. C. HOPMANS, S. SCHOUTEN, A. METS, W. I. C. RIJPSRA, AND J. S. SINNINGHE DAMSTÉ. 2011. Identification and distribution of intact polar branched tetraether lipids in peat and soil. *Org. Geochem.* **42**: 1007–1015, doi:10.1016/j.orggeochem.2011.07.006
- PITCHER, A., E. C. HOPMANS, S. SCHOUTEN, AND J. S. SINNINGHE DAMSTÉ. 2009. Separation of core and intact polar archaeal tetraether lipids using silica columns: Insights into living and fossil biomass contributions. *Org. Geochem.* **40**: 12–19, doi:10.1016/j.orggeochem.2008.09.008
- , L. VILLANUEVA, E. C. HOPMANS, S. SCHOUTEN, G.-J. REICHART, AND J. S. SINNINGHE DAMSTÉ. 2011. Niche segregation of ammonia-oxidizing archaea and anammox bacteria in the Arabian Sea oxygen minimum zone. *ISME J.* **5**: 1896–1904, doi:10.1038/ismej.2011.60
- QUESADA, C. A., J. LLOYD, L. O. ANDERSON, N. M. FYLLAS, M. SCHWARZ, AND C. I. CZIMCZIK. 2009. Soils of Amazonia with particular reference to the RAINFOR sites. *Biogeosciences* **8**: 1415–1440, doi:10.5194/bg-8-1415-2011
- SCHOUTEN, S., E. C. HOPMANS, M. BAAS, H. BOUMANN, S. STANDFEST, M. KÖNNEKE, D. A. STAHL, AND J. S. SINNINGHE DAMSTÉ. 2008. Intact membrane lipids of “*Candidatus Nitrosopumilus maritimus*,” a cultivated representative of the cosmopolitan mesophilic group I crenarchaeota. *Appl. Environ. Microbiol.* **74**: 2433–2440, doi:10.1128/AEM.01709-07
- , C. HUGUET, E. C. HOPMANS, M. V. M. KIENHUIS, AND J. S. SINNINGHE DAMSTÉ. 2007. Analytical methodology for TEX₈₆-paleothermometry by high-performance liquid chromatography/atmospheric pressure chemical ionization-mass spectrometry. *Anal. Chem.* **79**: 2940–2944, doi:10.1021/ac062339v
- , J. J. MIDDELBURG, E. C. HOPMANS, AND J. S. SINNINGHE DAMSTÉ. 2010. Fossilization and degradation of intact polar lipids in deep subsurface sediments: A theoretical approach. *Geochim. Cosmochim. Acta* **74**: 3806–3814, doi:10.1016/j.gca.2010.03.029
- SINNINGHE DAMSTÉ, J. S., J. OSSEBAAR, B. ABBAS, S. SCHOUTEN, AND D. VERSCHUREN. 2009. Fluxes and distribution of tetraether lipids in an equatorial African lake: Constraints on the application of the TEX86 palaeothermometer and BIT index in lacustrine settings. *Geochim. Cosmochim. Acta* **73**: 4232–4249, doi:10.1016/j.gca.2009.04.022
- , W. I. C. RIJPSRA, E. C. HOPMANS, J. W. H. WEIERS, B. U. FOESEL, J. OVERMANN, AND S. N. DEDYSH. 2011. 13,16-Dimethyl octacosanedioic acid (iso-diabolic acid), a common membrane-spanning lipid of Acidobacteria subdivisions 1 and 3. *Appl. Environ. Microbiol.* **77**: 4147–4154, doi:10.1128/AEM.00466-11
- , S. SCHOUTEN, E. C. HOPMANS, A. C. T. VAN DUIN, AND J. A. J. GEENEVAZEN. 2002. Crenarchaeol: The characteristic core glycerol dibiphytanyl glycerol tetraether membrane lipid of cosmopolitan pelagic crenarchaeota. *J. Lipid Res.* **43**: 1641–1651, doi:10.1194/jlr.M200148-JLR200
- STIOLI, H. 1984. The Amazon. Limnology and landscape ecology of a mighty tropical river and its basin. W. Junk.
- STURT, H. F., R. E. SUMMONS, K. SMITH, M. ELVERT, AND K. U. HINRICHS. 2004. Intact polar membrane lipids in prokaryotes and sediments deciphered by high-performance liquid chromatography/electrospray ionization multistage mass spectrometry—new biomarkers for biogeochemistry and microbial ecology. *Rapid Commun. Mass Spectrom.* **18**: 617–628.
- TIERNEY, J. E., AND J. M. RUSSELL. 2009. Distributions of brGDGTs in a tropical lake system: Implications for lacustrine application of the MBT-CBT paleoproxy. *Org. Geochem.* **40**: 1032–1036, doi:10.1016/j.orggeochem.2009.04.014

- , H. EGGERMONT, E. C. HOPMANS, D. VERSCHUREN, AND J. S. SINNINGHE DAMSTÉ. 2010. Environmental controls on branched tetraether lipid distributions in tropical East African lake sediments. *Geochim. Cosmochim. Acta* **74**: 4902–4918, doi:10.1016/j.gca.2010.06.002
- , S. SCHOUTEN, A. PITCHER, E. C. HOPMANS, AND J. S. SINNINGHE DAMSTÉ. 2012. Core and intact polar glycerol dialkyl glycerol tetraethers (GDGTs) in Sand Pond, Warwick, Rhode Island (USA): Insights into the origin of lacustrine GDGTs. *Geochim. Cosmochim. Acta* **77**: 561–581, doi:10.1016/j.gca.2011.10.018
- WALSH, E. M., A. E. INGALLS, AND R. G. KEIL. 2008. Sources and transport of terrestrial organic matter in Vancouver Island fjords and the Vancouver-Washington Margin: A multiproxy approach using $\delta^{13}\text{C}_{\text{org}}$, lignin phenols, and the ether lipid BIT index. *Limnol. Oceanogr.* **53**: 1054–1063, doi:10.4319/lo.2008.53.3.1054
- WEIJERS, J. W. H., B. BERNHARDT, F. PETERSE, J. P. WERNE, J. A. J. DUNGAIT, S. SCHOUTEN, AND J. S. SINNINGHE DAMSTÉ. 2011. Absence of seasonal patterns in MBT-CBT indices in mid-latitude soils. *Geochim. Cosmochim. Acta* **75**: 3179–3190, doi:10.1016/j.gca.2011.03.015
- , E. SCHEFUB, S. SCHOUTEN, AND J. S. SINNINGHE DAMSTÉ. 2007a. Coupled thermal and hydrological evolution of tropical Africa over the last deglaciation. *Science* **315**: 1701–1704, doi:10.1126/science.1138131
- , S. SCHOUTEN, O. C. SPAARGAREN, AND J. S. SINNINGHE DAMSTÉ. 2006. Occurrence and distribution of tetraether membrane lipids in soils: Implications for the use of the TEX_{86} proxy and the BIT index. *Org. Geochem.* **37**: 1680–1693, doi:10.1016/j.orggeochem.2006.07.018
- , J. C. VAN DEN DONKER, E. C. HOPMANS, AND J. S. SINNINGHE DAMSTÉ. 2007b. Environmental controls on bacterial tetraether membrane lipid distribution in soils. *Geochim. Cosmochim. Acta* **71**: 703–713, doi:10.1016/j.gca.2006.10.003
- , AND OTHERS. 2009. Constraints on the biological source(s) of the orphan branched tetraether membrane lipids. *Geomicrobiol. J.* **26**: 402–414, doi:10.1080/01490450902937293
- WHITE, D. C., W. M. DAVIS, J. S. NICKELS, J. D. KING, AND R. J. BOBBIE. 1979. Determination of the sedimentary microbial biomass by extractable lipid phosphate. *Oecologia* **40**: 51–62, doi:10.1007/BF00388810
- ZHU, C., J. W. H. WEIJERS, T. WAGNER, J. M. PAN, J. F. CHEN, AND R. D. PANCOST. 2011. Sources and distributions of tetraether lipids in surface sediments across a large river-dominated continental margin. *Org. Geochem.* **42**: 376–386, doi:10.1016/j.orggeochem.2011.02.002

Associate editor: Peter Hernes

Received: 02 April 2012
Accepted: 08 November 2012
Amended: 14 October 2012